Unconventional low-temperature features in the one-dimensional frustrated q-state Potts model

Yury Panov
Department of Theoretical and Mathematical Physics, Institute of Natural Sciences and Mathematics, Ural Federal University, 19 Mira Street, 620002 Ekaterinburg, Russia

Onofre Rojas
Department of Physics, Federal University of Lavras, 37200-900 Lavras, Minas Gerais, Brazil

(Received 12 March 2021; accepted 18 May 2021; published 2 June 2021)

Here we consider a one-dimensional q-state Potts model with an external magnetic field and an anisotropic interaction that selects neighboring sites that are in the spin state 1. The present model exhibits unusual behavior in the low-temperature region, where we observe an anomalous vigorous change in the entropy for a given temperature. There is a steep behavior at a given temperature in entropy as a function of temperature, quite similar to first-order discontinuity, but there is no jump in the entropy. Similarly, second derivative quantities like specific heat and magnetic susceptibility also exhibit strong acute peaks similar to second-order phase transition divergence, but once again there is no singularity at this point. Correlation length also confirms this anomalous behavior at the same given temperature, showing a strong and sharp peak which easily one may confuse with a divergence. The temperature where this anomalous feature occurs we call the pseudocritical temperature. We have analyzed physical quantities, like correlation length, entropy, magnetization, specific heat, magnetic susceptibility, and distant pair correlation functions. Furthermore, we analyze the pseudocritical exponents that satisfy a class of universality previously identified in the literature for other one-dimensional models; these pseudocritical exponents are for correlation length $\nu = 1$, specific heat $\alpha = 3$, and magnetic susceptibility $\mu = 3$.

DOI: 10.1103/PhysRevE.103.062107

I. INTRODUCTION

The advantage of exactly solvable models is their easy handling to analyze several properties, which can show interesting features despite it is simplicity. In contrast, more detailed models are rarely exactly solvable, and it would restrict us to performing only numerical computations, which prevents further analysis of these types of models. Some one-dimensional models [1] can help us understand and predict leading behavior in more complex models. From the experimental side, one-dimensional models accurately describe several chemical compounds [2,3]. That is why the one-dimensional models are quite important to investigate, both from theoretical and experimental points of view.

In the 1950s, van Hove [4] proposed a theorem to verify the absence of phase transition in uniform one-dimensional models with short-range interaction. The validity of the proposed theorem follows these conditions: (i) homogeneity, (ii) the Hamiltonian should not include particles positions terms (like external fields), and (iii) hard-core particles. Based on the Perron-Frobenius theorem [5], the van Hove theorem [4] is restricted to limited one-dimensional systems. Later, Cuesta and Sanchez [6] tried to extend the theorem of nonexistence phase transition for a more general one-dimensional system. Mainly, they included an external field and considered pointlike particles, which extend the theorem. Even with this extension, it is still far from being a fully general theorem of nonexistence phase transition.

There are unusual one-dimensional models with a short-range coupling that exhibit a phase transition at finite temperature. The zipper or Kittel model [7], which is one of the simplest models with a finite-size transfer matrix that exhibits a first-order phase transition. Another model, considered by Chui-Wicks [8], is typical of models called "solid on solid" for surface growth. It has the infinite dimension transfer matrix and is exactly solvable. Because of the impenetrable condition of the substrate, the model shows the existence of a finite-temperature phase transition. One more model is that considered by Dauxois-Peyrard [9], with an infinite-dimension transfer matrix, which can be explored numerically. Lately, Sarkanych *et al.* [10] proposed a one-dimensional Potts model with invisible states and short-range coupling. The term "invisible" means an additional energy degeneracy, which contributes only to the entropy but not the interaction energy. They named these states the invisible states, which generate the first-order phase transition.

Motivated by low-dimensional systems, such as the simple zipper model [7] that describes the long-chain nucleotides of deoxyribonucleic acid (DNA), Zimm and Bragg [11] introduced an essentially phenomenological cooperative parameter, which provides narrow helix-coil transitions. Since then, several investigations have been driven in the literature [12–15]. Cooperative systems in one dimension can be well represented by Potts-like models [12,14], where the helix-coil transition in polypeptides [13] can be studied, which is a typical application of theoretical physics to macromolecular systems, the results of which are quite appropriate to understanding the physical properties of the helix-coil transition. The polycyclic aromatic surface elements of the carbon

nanotube (CNT) and the aromatic DNA provide reversible adsorption. Tonoyan *et al.* [15] adapted the Hamiltonian of the zipper model in order to take into account the DNA-CNT interactions.

The Potts model is a generalization of the Ising model to more than two components, such as interacting spins in a crystalline lattice. The standard q-state Potts model [16] with $q \geqslant 2$ has been assumed as an integer denoting the number of states of each site. The Potts model is quite relevant in statistical physics. In some crystal lattices vacancies would occur, which lead to a site diluted Potts model. The site diluted q-state Potts model [17,18] is equivalent to $(q+1)$-state standard Potts model [16]. Chaves and Riera [19] investigated a particular case of dilute Potts chain. Recently, a different dilute Ising spin-1 chain [20] was also studied in the framework of the projection operator.

An unusual property called pseudotransition was observed in some recent works, like in a double-tetrahedral chain of localized Ising spins with mobile electrons showing a strong thermal excitation that easily suggests the existence of a first-order phase transition [21,22]. Similarly, the frustrated spin-1/2, Ising-Heisenberg's three-leg tube exhibited a pseudotransition [23]. In Ref. [24], this property was also observed when studying the specific heat, wherein a sharp peak on the spin-1/2 Ising-Heisenberg ladder with alternating Ising and Heisenberg interleg couplings was reported. This weird property was even observed in the spin-1/2 Ising diamond chain in the neighborhood of the pseudotransition [25]. Deeper investigations were performed on this peculiar property in Ref. [26]. Additionally, the distant correlation functions have been studied around the pseudotransition for a spin-1/2 Ising-XYZ diamond chain [27]. A slightly different proposal to identify the pseudotransition in one-dimensional models [28] was explored in the framework of the phase boundary residual entropy relationship with the finite-temperature pseudotransition. Further investigation around the pseudotransition was also focused on the universality and pseudocritical exponents of one-dimensional models [29].

We organize the article as follows. In Sec. II, we present the model and analyze the zero-temperature phase diagrams. In Sec. III, we study the thermodynamics of the model and explore an anomalous phenomenon called pseudotransition for several physical quantities. In Sec. IV, we investigate the manifest of the pseudotransition in terms of the distant pair correlation functions and correlation length. The pseudocritical exponents for the correlation length, specific heat, and susceptibility we discuss in Sec. V. Finally, in Sec. VI, we present our conclusions.

II. THE FRUSTRATED POTTS CHAIN

Let us consider a Potts model [16]; here we assume the one-dimensional case, whose Hamiltonian becomes

$$H = -\sum_{i=1}^{N} \left\{ J\delta_{\sigma_i,\sigma_{i+1}} + K\delta_{\sigma_i,1}\delta_{1,\sigma_{i+1}} + h\delta_{\sigma_i,1} \right\}, \tag{1}$$

with $\sigma = \{1, \ldots q\}$. Whereas J is bound coupling parameter, h denotes the external field aligned to state 1, and K denotes the parameter of an anisotropic interaction that selects neighboring sites that are in the spin state 1.

The Hamiltonian (1) for the case $q = 2$, like the standard Potts model, drops into the spin-1/2 Ising chain model. For the case of $q \geqslant 3$, the model becomes a frustrated system for certain choices of parameters, as shown below.

It is worth noticing that the Hamiltonian (1) can also be equivalent to a diluted Potts model with $q-1$ states, as demonstrated by Wu [16]. The features of the critical properties of the two-dimensional diluted Potts model were studied earlier using Fortuin-Kasteleyn clusters [30] and the transfer matrix method [31].

A. Zero-temperature phase diagram

In order to analyze the phase diagram of q-state Potts model at zero temperature, we identify four ground states assuming $q \geqslant 3$ for the model (1), which read

$$|FM_1\rangle = \prod_{i=1}^{N} (|1\rangle_i), \tag{2}$$

$$|FM_2\rangle = \prod_{i=1}^{N} (|j\rangle_i), \quad j = \{2, \ldots, q\}, \tag{3}$$

$$|FR_1\rangle = \prod_{i=1}^{N/2} (|1\rangle_{2i-1}|\sigma_i\rangle_{2i}), \tag{4}$$

$$|FR_2\rangle = \prod_{i=1}^{N} (|\sigma_i\rangle), \quad \sigma_i \neq \sigma_{i\pm1}, \tag{5}$$

where $\sigma_i = \{2, \ldots, q\}$. Additional information, concerning phases and phase boundaries, are listed in Table I for different physical quantities at zero temperature, like magnetization, entropy, and pair distribution functions (PDF), which can be obtained by taking the limit of $T \to 0$ of the quantities (23), (55), and (67).

Figure 1(a) illustrates schematically the ground-state phase diagram in the plane J-h, for the Hamiltonian (1) assuming $K < 0$. Here we observe four phases illustrated above. Similarly, Figs. 1(b) and 1(c) illustrate alternative phase diagrams for $K = 0$ and $K > 0$, respectively.

The first state is a type of ferromagnetic (FM_1) phase where all sites are in state $\sigma_i = 1$, with energy per spin $E_{FM_1} = -(J + K + h)$. The second state is another type of ferromagnetic (FM_2) phase with energy $E_{FM_2} = -J$. The average fraction of pairs of adjacent spins in the same state μ, where $\mu = 2, \ldots, q$, is PDF $g^{(1)}_{\mu,\mu} = 1/(q-1)$ (see Table 1). At the same time, $g^{(1)}_{\mu,\mu'} = 0$, where $\mu \neq \mu'$, which means that in the thermodynamic limit, the fraction of pairs with different spin states and their contribution to the energy of the system are equal to zero. This implies that, in the general case, the FM_2 phase consists of $q-1$ sorts of equivalent macroscopic ferromagnetic domains with spins in the μ state. Equation (3) corresponds to the single-domain case. The entropy of both FM_1 and FM_2 phases is zero. The third is a frustrated type (FR_1) phase, with alternating sites are in states $\sigma_{2i-1} = 1$, while the other sites σ_{2i} can take $\sigma_{2i} = 2, \ldots, q$, and the corresponding energy is $E_{FR_1} = -h/2$. This phase state is frustrated at $q > 2$. Because every second site

TABLE I. The nearest neighbor pair distribution functions $g^{(1)}_{\mu,\mu'}$, $\mu, \mu' = 2, \ldots, q$, magnetization m_1, and entropy $\mathcal{S}$ of the frustrated Potts chain at zero temperature. Here $q_1 = \sqrt{4q-3}$, $q_2 = \sqrt{(q-1)(q+3)}$, $q_3 = 1+\sqrt{q-1}$, and $q_4 = \sqrt{(q-1)^2+4}$.

GS phase	$g^{(1)}_{1,1}$	$g^{(1)}_{\mu,\mu}$	$g^{(1)}_{1,\mu}$	$g^{(1)}_{\mu,\mu'}$	m_1	$\mathcal{S}$
FM_1	1	0	0	0	1	0
FM_2	0	$\frac{1}{q-1}$	0	0	0	0
FR_1	0	0	$\frac{1}{2(q-1)}$	0	$\frac{1}{2}$	$\frac{1}{2}\ln(q-1)$
FR_2	0	0	0	$\frac{1}{(q-1)(q-2)}$	0	$\ln(q-2)$
FR_1-FM_1	$\frac{1}{q_1}$	0	$\frac{q_1-1}{2q_1(q-1)}$	0	$\frac{2q-1+q_1}{q_1(1+q_1)}$	$\ln\frac{1+q_1}{2}$
FR_2-FM_2	0	$\frac{1}{(q-1)^2}$	0	$\frac{1}{(q-1)^2}$	0	$\ln(q-1)$
FR_1-FR_2	0	0	$\frac{1}{q(q-1)}$	$\frac{1}{q(q-1)}$	$\frac{1}{q}$	$\ln(q-1)$
FR_1-FM_2 ($K<0$)	0	$\frac{1}{q_1(q-1)}$	$\frac{q_1-1}{2q_1(q-1)}$	0	$\frac{2q-2}{q_1(1+q_1)}$	$\ln\frac{1+q_1}{2}$
FR_2-FM_1 ($K>0$)	0	0	0	$\frac{1}{(q-1)(q-2)}$	0	$\ln(q-2)$
FM_1-FM_2 ($K>0$)	0	$\frac{1}{q-1}$	0	0	0	0
FM_1-FM_2 ($K=0$)	$\frac{1}{q}$	$\frac{1}{q}$	0	0	$\frac{1}{q}$	0
FM_1-FM_2 ($K<0$)	$\frac{1}{2}$	$\frac{1}{2(q-1)}$	0	0	$\frac{1}{2}$	0
Q_1	0	$\frac{1}{q_2(q-1)}$	$\frac{2}{q_2(q-1+q_2)}$	$\frac{1}{q_2(q-1)}$	$\frac{2}{q+3+q_2}$	$\ln\frac{q-1+q_2}{2}$
Q_2	$\frac{1}{2q_3}$	$\frac{1}{2q_3(q-1)}$	$\frac{1}{2q_3\sqrt{q-1}}$	0	$\frac{1}{2}$	$\ln q_3$
P_1	$\frac{3-q+q_4}{q_4(q-1+q_4)}$	0	$\frac{2}{q_4(q-1+q_4)}$	$\frac{q-3+q_4}{q_4(q-1)(q-1+q_4)}$	$\frac{q+1+q_4}{q_4(q-1+q_4)}$	$\ln\frac{q-1+q_4}{2}$
P_2	0	$\frac{1}{(q-1)^2}$	0	$\frac{1}{(q-1)^2}$	0	$\ln(q-1)$
S	$\frac{1}{q^2}$	$\frac{1}{q^2}$	$\frac{1}{q^2}$	$\frac{1}{q^2}$	$\frac{1}{q}$	$\ln q$

can be in any of the $q-1$ states, the entropy per spin is equal to $\mathcal{S} = \frac{1}{2}\ln(q-1)$. The fourth state is another type of frustrated (FR_2) phase; in each site σ_i can take independently $\sigma_i = \{2, \ldots, q\}$ but $\sigma_i \neq \sigma_{i\pm1}$, whose corresponding energy is $E_{FR_2} = 0$. In this case, each subsequent site of the chain can be in one of $q-2$ states, and the entropy is equal to $\mathcal{S} = \ln(q-2)$. If $q > 3$, the FR_2 phase is evidently frustrated state. However, for $q = 3$, there is an alternation of sites in states $\sigma_i = 2$ and $\sigma_i = 3$, and the entropy of the FR_2 phase is zero.

It is important to note that two different situations can occur at phase boundaries. The first case is when the states of two adjacent phases are mixed at the microscopic level. For example, for the FR_1-FM_1 boundary, the FR_1 state of any pair of sites can be changed to the FM_1 state, and vice versa. Such a replacement does not lead to the appearance of microscopic states from other phases, and the energy of the system does not change. As a result, the entropy of such a mixed state at the phase boundary is greater than the entropy of the adjacent phases. A similar situation is observed for the boundaries FR_1-FR_2, FR_2-FM_2, and FR_1-FM_2 at $K < 0$. In the second case, it can be a pure state of one of the adjacent phases, or the phase separation, when each phase is represented by the macroscopic domains. So, on the FR_2-FM_1 boundary for $K > 0$, the replacement for a pair of neighboring nodes in state FR_2 by state FM_1 leads to the appearance of FR_1 states, which are energetically unfavorable. A similar situation occurs at the FM_1-FM_2 boundary. Note that in the FM_1-FM_2 interface curve the residual entropy is zero.

III. THERMODYNAMICS

The frustrated q-state Potts model Hamiltonian (1) can be solved through transfer matrix technique, which results in a

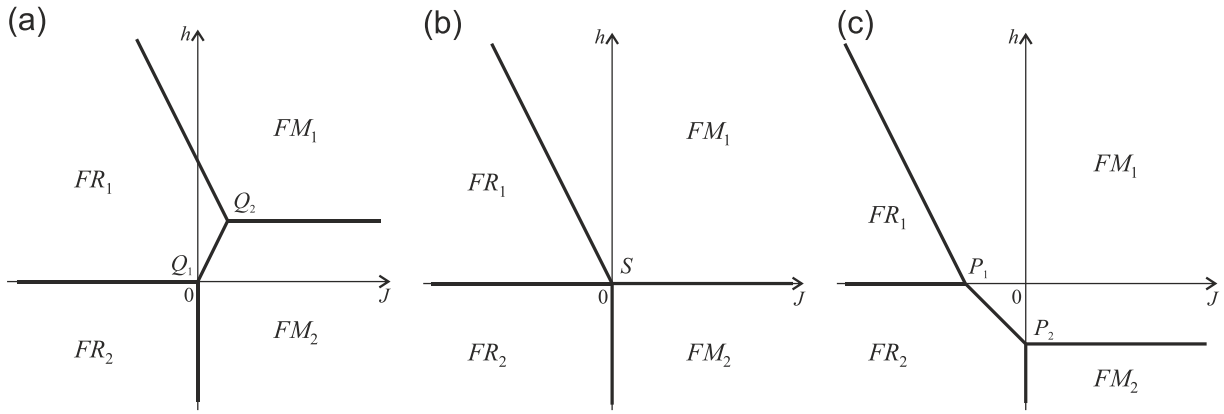

FIG. 1. The ground-state phase diagrams of the q-state Potts chain with Hamiltonian (1) for $q \geqslant 3$. (a) $K < 0$, (b) $K = 0$, and (c) $K > 0$. Here the points are $Q_1(0, 0)$, $Q_2(-K/2, -K)$, $S(0, 0)$, $P_1(-K, 0)$, and $P_2(0, -K)$.

q-dimensional matrix, given by

$$\mathbf{V} = \begin{pmatrix} d_1 & t_1 & t_1 & \cdots & t_1 & t_1 \\ t_1 & d_2 & t_2 & \cdots & t_2 & t_2 \\ t_1 & t_2 & d_2 & \cdots & t_2 & t_2 \\ \vdots & \vdots & \vdots & \ddots & \vdots & \vdots \\ t_1 & t_2 & t_2 & \cdots & d_2 & t_2 \\ t_1 & t_2 & t_2 & \cdots & t_2 & d_2 \end{pmatrix}, \tag{6}$$

where $d_1 = xkz$, $d_2 = x$, $t_1 = \sqrt{z}$, $t_2 = 1$, and $x = e^{\beta J}$, $k = e^{\beta K}$, and $z = e^{\beta h}$.

Let us write the transfer matrix eigenvalues similarly to those defined in Ref. [26], and so we have

$$\lambda_1 = \tfrac{1}{2}\big(w_1 + w_{-1} + \sqrt{(w_1 - w_{-1})^2 + 4w_0^2}\big), \tag{7}$$

$$\lambda_2 = \tfrac{1}{2}\big(w_1 + w_{-1} - \sqrt{(w_1 - w_{-1})^2 + 4w_0^2}\big), \tag{8}$$

$$\lambda_j = d_2 - t_2, \quad j = \{3, 4, \ldots, q\}, \tag{9}$$

where

$$w_1 = d_1, \tag{10}$$

$$w_{-1} = d_2 + (q-2)t_2, \tag{11}$$

$$w_0 = \sqrt{q-1}\, t_1. \tag{12}$$

The corresponding transfer matrix eigenvectors are

$$|u_1\rangle = \cos(\phi)|1\rangle + \frac{\sin(\phi)}{\sqrt{q-1}} \sum_{\mu=2}^{q} |\mu\rangle, \tag{13}$$

$$|u_2\rangle = -\sin(\phi)|1\rangle + \frac{\cos(\phi)}{\sqrt{q-1}} \sum_{\mu=2}^{q} |\mu\rangle, \tag{14}$$

$$|u_j\rangle = \sqrt{\frac{j-2}{j-1}}\left(\frac{1}{j-2}\sum_{\mu=2}^{j-1}|\mu\rangle - |j\rangle\right), \quad j = \{3, \ldots, q\}, \tag{15}$$

where $\phi = \frac{1}{2}\cot^{-1}(\frac{w_1 - w_{-1}}{2w_0})$, with $-\frac{\pi}{4} \leqslant \phi \leqslant \frac{\pi}{4}$.

By using the transfer matrix eigenvalues, we express the partition function as follows:

$$\begin{aligned} Z_N &= \lambda_1^N + \lambda_2^N + (q-2)\lambda_3^N \\ &= \lambda_1^N \left\{1 + \left(\frac{\lambda_2}{\lambda_1}\right)^N + (q-2)\left(\frac{\lambda_3}{\lambda_1}\right)^N\right\}. \end{aligned} \tag{16}$$

It is evident that the eigenvalues satisfy the following relation $\lambda_1 > \lambda_2 \geqslant \lambda_3$. Hence, assuming q is finite, the free energy per spin in thermodynamic limit reduces to

$$f = -T \ln(\lambda_1). \tag{17}$$

Note that the free energy is a continuous function with no singularity or discontinuity, and thus we do not expect any real phase transition at finite temperature.

A. Pseudocritical temperature

Recently pseudocritical temperature has been discussed in Ising and Ising-Heisenberg spin models [21,23,24,26], in several one-dimensional spin models.

To find pseudocritical temperature, we follow the same strategy to that used in Ref. [26]. In our case, the largest eigenvalues has the same structure as that found in Ref. [26], so necessary conditions for a pseudotransition are met, if $w_1 \sim w_{-1} \ggg w_0$, $|w_1 - w_{-1}| \gg w_0$. The pseudotransition point can be obtained when the first term inside the square root of λ_1 given by Eq. (7) turns to zero, which gives

$$e^{\frac{J+K+h}{T_p}} = q - 2 + e^{\frac{J}{T_p}}. \tag{18}$$

In principle, using the above relation, one can find the critical temperature as a function of some Hamiltonian parameters.

The q-state Potts chain does not exhibit a real spontaneous long-range order at finite temperature since its one-dimensional character. Therefore, we define a term "quasi" to refer low-temperature regions mainly dominated by ground-state configuration. Hence, FR_2 in a low-temperature region is called as qFR_2, and so on. As shown in Ref. [28], pseudotransitions occur for states near those phase boundaries whose residual entropy is a continuous function of the model parameters for at least one of the adjacent phases. As discussed earlier, the state of the FR_2-FM_1 boundary coincides with the FR_2 state, so for the qFR_2-qFM_1 boundary, we get from Eq. (18) the following relation,

$$e^{\frac{K+h}{T_p}} = e^{-\frac{J}{T_p}}(q-2) + 1, \tag{19}$$

which we can simplify and write approximately in the form

$$T_p = \frac{J + K + h}{\ln(q-2)}. \tag{20}$$

This is the known expression [21,23,26,28] for the pseudotransition temperature:

$$E_{\mathrm{FM}_1} - E_{\mathrm{FR}_2} = T_p(\mathcal{S}_{\mathrm{FR}_2} - \mathcal{S}_{\mathrm{FM}_1}), \tag{21}$$

where the energy and entropy per unit cell are given at zero temperature. Since $E_{\mathrm{FM}_1} = E_{\mathrm{FR}_2}$ at the qFR_2-qFM_1 boundary, T_p tends to zero near to it.

Another phase boundary we focus on is qFM_2-qFM_1. It is worth mentioning that the entropy of the FM_1 and FM_2 phases is zero, so the entropy is a continuous function for both adjacent phases. For the qFM_2-qFM_1 boundary, Eq. (18) can be approximately written in the following form:

$$\frac{1}{T_p}(K + h)e^{J/T_p} = q - 2. \tag{22}$$

In Fig. 2(a) is reported the density plot of entropy in the plane T-h, assuming fixed parameters $K = 1$, $J = -0.5$. Dashed curve describes the boundary qFR_2-qFM_1, which corresponds to the pseudocritical temperature T_p as a function of h, according to Eq. (19). It can be seen that the curve is an almost straight line well represented by (20). We can observe also how the sharp boundary between quasiphase melts smoothly for higher temperature. Similar density plot is depicted in Fig. 2(b) for the magnetization m_1 in the plane T-h for the same set of parameters as in Fig. 2(a). Analogously, we analyze the phase boundary between qFM_2-qFM_1 in Fig. 2(c), assuming fixed parameters $K = 1$, $J = 0.99$, and $T = 0.01$. The dashed line is given by Eq. (19) and nicely approximated by (22), and since there is no residual entropy in the boundary the quasiphases qFM_1 and qFM_2 lead to zero when temperature vanishes; by looking at entropy we cannot distinguishes the boundaries of the quasiphases. However, in Fig. 2(d) we

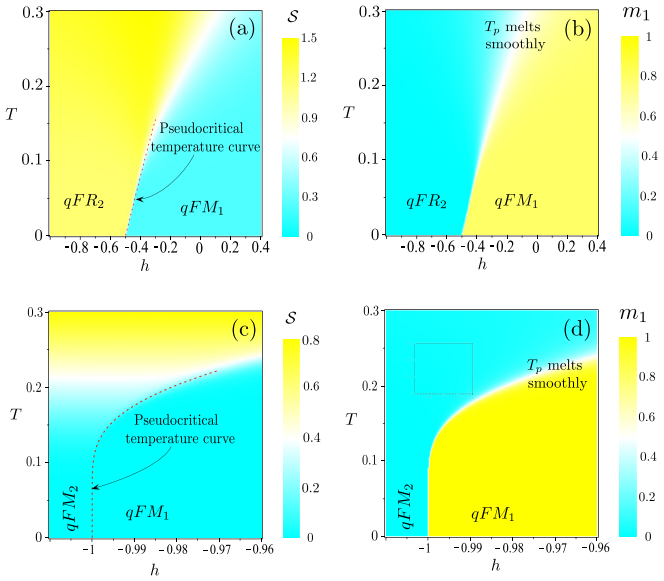

FIG. 2. Density plot (a) for entropy in the plane T-h, for $K = 1$ and $J = -0.5$. (b) Magnetization m_1 for the same set of parameters as in panel (a). In panel (c), entropy in the plane T-h for fixed $K = 1$, $J = 0.99$. In panel (d), magnetization for the same set of parameters as in panel (c).

illustrate the density plot of magnetization m_1 for the same set of parameters in Fig. 2(c), and we observe clearly a sharp boundary between qFM_1 and qFM_2 regions. This boundary melts smoothly as soon as temperature increases.

B. Entropy and specific heat

The entropy and the specific heat of the system can be obtained from the free energy (17) by

$$\mathcal{S} = -\frac{\partial f}{\partial T}, \quad C = -T\frac{\partial^2 f}{\partial T^2}. \tag{23}$$

Of particular interest is the behavior of thermodynamic characteristics near the pseudotransition point. The general method for considering this issue was developed in Ref. [29]. For the one-dimensional Potts model, it is possible to find an explicit form of approximation of the free energy and other thermodynamic quantities near T_p. Assuming that $\tau = (T - T_p)/T_p \ll 1$ and taking into account Eq. (18), we can write

$$w_1 = e^{\beta(J+K+h)} = \tilde{w}_1^{\frac{1}{1+\tau}} \approx \tilde{w}_1(1 - \ln \tilde{w}_1\, \tau), \tag{24}$$

$$w_{-1} = q - 2 + e^{\beta J} = q - 2 + x_p^{\frac{1}{1+\tau}} \approx \tilde{w}_1 - x_p \ln x_p\, \tau, \tag{25}$$

where

$$\tilde{w}_1 = w_1|_{\tau=0} = q - 2 + x_p, \tag{26}$$

and we define the parameters $x_p = e^{J/T_p}$ and $k_p = e^{K/T_p}$. The value of $w_1 - w_{-1}$ is zero at $\tau = 0$ due to Eq. (18), so we get

$$w_1 - w_{-1} \approx -\tilde{w}_1\, a\, \tau, \tag{27}$$

where we introduce the parameter a as

$$a = \ln \tilde{w}_1 - \frac{x_p \ln x_p}{\tilde{w}_1}. \tag{28}$$

Note that the parameter a^{-1} define the slope of the pseudotransition curve in the plane T-h [see Figs. 2(a) and 2(c)], $dT_p/dh = a^{-1}$.

The condition $|w_1 - w_{-1}| \gg w_0$ which is met in the vicinity of T_p causes quasisingular behavior of the derivative of square root in Eqs. (7) and (8) at $\tau = 0$. Assuming this is the case, we can write the approximation

$$4w_0^2 = 4(q-1)e^{\beta h} \approx 4(q-1)\frac{\tilde{w}_1}{x_p k_p}. \tag{29}$$

This allows us to write eigenvalues (7) and (8) near $\tau = 0$ as

$$\lambda_{1,2} \approx \tilde{w}_1\big[1 + \big(\tfrac{1}{2}a\tau - \ln \tilde{w}_1\big)\tau \pm \tfrac{1}{2}\sqrt{a^2\tau^2 + b^2}\big], \tag{30}$$

where $b^2 = 4w_0^2/\tilde{w}_1^2$, and yields the approximation for the free energy (17) in the vicinity of T_p:

$$f \approx -T_p\big[\ln \tilde{w}_1 - \tfrac{1}{2}a\tau + \tfrac{1}{2}\sqrt{a^2\tau^2 + b^2}\big]. \tag{31}$$

The expressions (30) and (31), being exact at $\tau = 0$, have a small deviation from rigorous expansions of $\lambda_{1,2}$ and f in the tiny vicinity $0 < |\tau| < \ln(x_p k_p)\, b^2/a^2 \lll 1$ due to the neglect of linear terms in Eq. (29), but well approximate the functions $\lambda_{1,2}$ and f at $\ln(x_p k_p)\, b^2/a^2 < |\tau| \ll 1/|\ln x_p|$. This implies a simple necessary condition for a pseudotransition in the form $b/a \ll T_p/|J|$.

For the entropy in the same region of τ, using (23), we obtain the following expression:

$$\mathcal{S} \approx \frac{a}{2}\left(1 + \frac{a\tau}{\sqrt{a^2\tau^2 + b^2}}\right). \tag{32}$$

Equation (32) describes the entropy jump in a small vicinity of T_p,

$$\Delta\mathcal{S}_p = \mathcal{S}\left(\tau > \frac{b}{a}\right) - \mathcal{S}\left(\tau < -\frac{b}{a}\right) = a, \tag{33}$$

which may be related to the "latent heat" of pseudotransition, $Q = T_p \Delta\mathcal{S}_p = aT_p$.

Second derivation of Eq. (31) by temperature gives the approximation of the specific heat near T_p,

$$C \approx \frac{a^2 b^2}{2(a^2\tau^2 + b^2)^{\frac{3}{2}}}. \tag{34}$$

This allows us to estimate the maximum value of the specific heat in T_p as

$$C_p = \tfrac{1}{2}a^2 b^{-1}. \tag{35}$$

We can qualify the peak of the specific heat near T_p by its half-width at half-maximum Ψ_τ. From (34), we find that $\Psi_\tau = \gamma b/a$, where $\gamma = \sqrt{2^{2/3} - 1} \approx 0.7664$, and hence $\Psi_\tau \ll 1$ due to a necessary condition for a pseudotransition.

The entropy and specific heat of the qFM_1 states having $q = 5$, $J = -0.5$, $K = 1$ in a given external field h are shown in Figs. 3(a) and 3(b). At sufficiently low temperatures, the qFR_2-qFM_1 pseudotransition is observed, which is

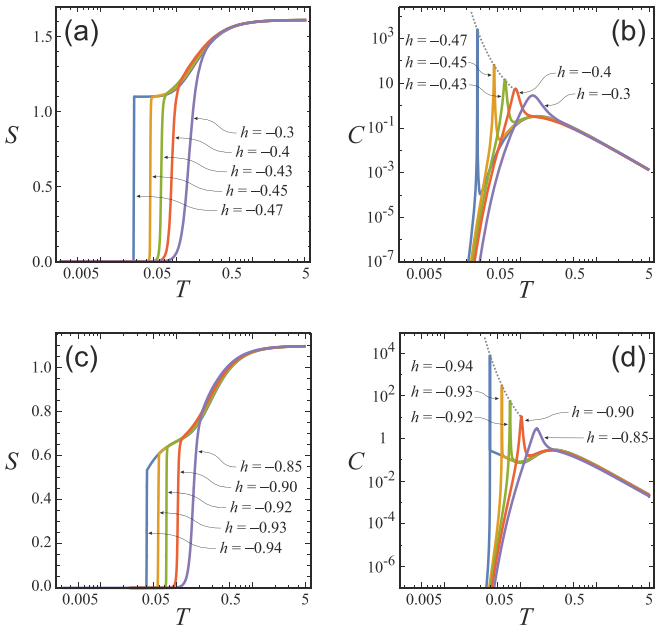

FIG. 3. The entropy and specific heat of the qFM_1 states near the FR_2-FM_1 boundary [(a), (b)] with $q = 5$, $J = -0.5$, $K = 1$, and [(c), (d)] with $q = 3$, $J = -0.05$, $K = 1$, in an external field h. The dotted lines in panels (b) and (d) show the magnitude of C_p at $T = T_p$ given by Eqs. (37) and (39) respectively.

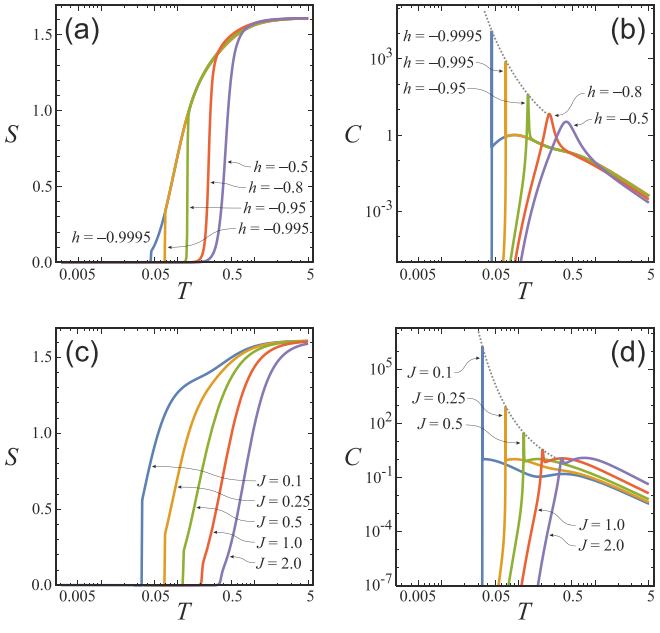

FIG. 4. The entropy and specific heat of the qFM_1 states near the FM_1-FM_2 boundary [(a), (b)] with $q = 5$, $J = 0.25$, $K = 1$ in an external field h, and [(c), (d)] with $q = 5$, $h = -0.995$, $K = 1$ for the different values of the coupling parameter J. The dotted lines in panels (b) and (d) show the magnitude of C_p at $T = T_p$ given by Eq. (41).

accompanied by a jump in entropy and a narrow peak in the specific heat.

For the qFR_2-qFM_1 transition at $q > 3$, the condition $x_p \ll q - 2$ is met, since $J < 0$ and $|J|/T_p \gg 1$, so approximately

$$a = \ln(q-2), \quad b = 2\sqrt{\frac{q-1}{(q-2)x_p k_p}}. \tag{36}$$

The entropy jump $\Delta\mathcal{S}_p = \ln(q-2)$ equals the residual entropy of the qFR_2 phase (see Table I). An expression for the maximum value of the specific heat,

$$C_p = \frac{\ln^2(q-2)}{4}\sqrt{\frac{q-2}{q-1}}\, e^{\frac{K-|J|}{2T_p}}, \tag{37}$$

shows that C_p decreases for the states close to the point P_1 in Fig. 1(c). The magnitudes of the specific heat peaks (37) are shown in Fig. 3(b) with dotted lines. It is interesting to note that $C_p\Psi_\tau = \frac{1}{2}\gamma\ln(q-2) = \text{const}(T_p)$, so, having a finite height, the specific heat peak tends to the δ function near the FR_2-FM_1 boundary with the T_p lowering.

In Figs. 3(c) and 3(d), the entropy and specific heat of the qFM_1 states having $q = 3$, $J = -0.05$, and $K = 1$ in a given external field h are shown. The case $q = 3$ is special, since the residual entropy of the FR_2-FM_1 boundary is a continuous function for both adjacent phases. For the parameter a, we obtain

$$a = (1 - \ln x_p)x_p, \tag{38}$$

so the necessary condition for a pseudotransition $b/a \propto e^{(3|J|-K)/2T_p} \ll T_p/|J|$ is met if $K > 3|J|$. Since in this case $J < 0$, the entropy jump (33) drops with decreasing of T_p due to the exponent in $x_p = e^{J/T_p}$, as can be seen from Fig. 3(c). A maximal value of the specific heat in T_p approximately has the following form:

$$C_p = \frac{(1 - J/T_p)^2}{4\sqrt{2}}\, e^{\frac{K-5|J|}{2T_p}}. \tag{39}$$

From (39) we may conclude that if $K > 5|J|$ the pseudotransition is accompanied with exponentially high peak of the specific heat. From a general point of view, this issue was discussed in detail in Ref. [28].

Figure 4 shows the temperature dependencies of the entropy and specific heat for states having parameters close to the FM_1-FM_2 boundary for $K = 1$. One set of states, shown in Figs. 4(a) and 4(b), has $J = 0.25$ and different values of the external field h, and the states in another set, shown in Figs. 4(c) and 4(d), have the same h and differ in the coupling constant J.

Near the FM_1-FM_2 boundary, for which the residual entropy is zero, as for both adjacent phases, we get

$$a = (q-2)\frac{1 + \ln x_p}{x_p}, \quad b = \frac{2}{x_p}\sqrt{\frac{q-1}{k_p}}. \tag{40}$$

The condition for a pseudotransition $b/a \propto e^{-K/2T_p} \ll T_p/|J|$ will be met only if $K > 0$. In this case $J > 0$, so the entropy jump $\Delta\mathcal{S}_p = a \propto e^{-J/T_p}$ decreases exponentially with decreasing T_p. This effect is shown in Fig. 4(a). The specific heat in T_p approximately is given by

$$C_p = \frac{(q-2)^2(1 + J/T_p)^2}{4\sqrt{q-1}}\, e^{\frac{K-2J}{2T_p}}. \tag{41}$$

Equation (41) shows that for $K > 2J$ the qFM$_2$-qFM$_1$ pseudotransition entails an exponentially high peak of the specific heat if the pseudotransition temperature is small enough. The decrease in the peak of the specific heat near T_p with increasing J is shown in Fig. 4(d).

C. Magnetization and magnetic susceptibility

It is important to study the magnetization property of the present model. In order to obtain a general average $\langle\delta_{\sigma,\mu}\rangle$, let us define the following operator:

$$\boldsymbol{m}_\mu = \sum_{j=1}^{q} \delta_{j,\mu}|j\rangle\langle j| = |\mu\rangle\langle\mu|. \tag{42}$$

Therefore, the average of $\boldsymbol{m}_\mu$ becomes

$$\langle\delta_{\sigma,\mu}\rangle = m_\mu = Z_N^{-1}\,\mathrm{tr}(\boldsymbol{m}_\mu \mathbf{V}^N). \tag{43}$$

Expressing Eq. (42) in the eigenstate basis given in Eqs. (13)–(15), we have

$$\tilde{\boldsymbol{m}}_\mu = \sum_{j_1,j_2=1}^{q} \langle u_{j_1}|\boldsymbol{m}_\mu|u_{j_2}\rangle |u_{j_1}\rangle\langle u_{j_2}|, \tag{44}$$

with

$$\langle u_{j_1}|\boldsymbol{m}_\mu|u_{j_2}\rangle = \langle u_{j_1}|\mu\rangle\langle\mu|u_{j_2}\rangle, \tag{45}$$

and denoting $\langle\mu|u_j\rangle = c_{\mu,j}$, we can write (44) as

$$\tilde{\boldsymbol{m}}_\mu = \sum_{j_1,j_2=1}^{q} c^*_{\mu,j_1} c_{\mu,j_2} |u_{j_1}\rangle\langle u_{j_2}|. \tag{46}$$

In a similar way, the transfer matrix in eigenstate basis (13)–(15) becomes

$$\tilde{\mathbf{V}} = \sum_{j=1}^{q} \lambda_j |u_j\rangle\langle u_j|. \tag{47}$$

Hence, substituting (46) and (47) into Eq. (43), we obtain

$$m_\mu = \frac{1}{Z_N}\sum_{j_1=1}^{q}\langle u_{j_1}| \sum_{j_2,j_3=1}^{q} c^*_{\mu,j_2} c_{\mu,j_3} |u_{j_2}\rangle\langle u_{j_3}|\lambda_{j_3}^N|u_{j_1}\rangle. \tag{48}$$

In the thermodynamic limit ($N \to \infty$) we can simplify (48). Therefore, if we write the magnetization m_μ in terms of $c_{\mu,j}$, it reduces to

$$m_\mu = c^*_{\mu,1} c_{\mu,1} = |c_{\mu,1}|^2. \tag{49}$$

The explicit expression of coefficients are given by

$$c_{1,1} = \cos\phi, \quad c_{\mu,1} = \frac{\sin\phi}{\sqrt{q-1}}, \tag{50}$$

$$c_{1,2} = -\sin\phi, \quad c_{\mu,2} = \frac{\cos\phi}{\sqrt{q-1}}, \tag{51}$$

where $\mu = \{2,\ldots,q\}$.

Analogously, the remaining coefficients are written by

$$c_{\mu,j} = \begin{cases} 0; & \mu = \{1, j+1, \ldots, q\} \\ \frac{1}{\sqrt{(j-1)(j-2)}}; & \mu = \{2,\ldots,j-1\} \\ -\sqrt{\frac{j-1}{j-2}}; & \mu = j \end{cases}, \tag{52}$$

where we consider $j = \{3,\ldots,q\}$.

As a consequence, we can get the magnetization by using (50) in (49), which becomes

$$m_1 = \cos^2\phi, \quad m_\mu = \frac{\sin^2\phi}{q-1}. \tag{53}$$

Additionally, from the above result, we get the following identity:

$$m_1 + (q-1)m_\mu = 1, \quad \mu = \{2,\ldots,q\}. \tag{54}$$

Alternatively one can obtain m_1 taking the derivative of free energy with respect to external field h,

$$m_1 = \langle\delta_{\sigma,1}\rangle = -\frac{\partial f}{\partial h}, \tag{55}$$

and m_μ we can obtain from (54).

On the other hand, the magnetic susceptibility χ_1 can be obtained by deriving (55), which results in

$$\chi_1 = \frac{1}{4T}\sin(2\phi)^3\left(\frac{d_1 + d_2 + (q-2)t_2}{2t_1\sqrt{q-1}}\right), \tag{56}$$

Similarly, one can obtain for $\mu = \{2,\ldots,q\}$,

$$\chi_\mu = \frac{\partial m_\mu}{\partial h}, \tag{57}$$

and we have the following relation,

$$\chi_\mu = -\frac{1}{q-2}\chi_1, \tag{58}$$

for $\mu = \{2,\ldots,q\}$.

To find an approximate expression for the magnetization near T_p, we can write it by using Eqs. (17) and (55) in the form

$$m_1 = \frac{T}{\lambda_1}\frac{\partial\lambda_1}{\partial h}. \tag{59}$$

When calculating the derivative with respect to h, we take into account that $\frac{\partial}{\partial h}w_1 = \beta w_1$, $\frac{\partial}{\partial h}w_{-1} = 0$, $\frac{\partial}{\partial h}w_0^2 = \beta w_0^2$, and obtain

$$m_1 = \frac{1}{2\lambda_1}\left(w_1 + \frac{(w_1 - w_{-1})w_1 + 2w_0^2}{(w_1 - w_{-1})^2 + 4w_0^2}\right). \tag{60}$$

Using Eqs. (24)–(29) and leaving only the leading terms, we find an approximation for m_1 in the following form:

$$m_1 \approx \frac{1}{2}\left(1 - \frac{a\tau}{\sqrt{a^2\tau^2 + b^2}}\right). \tag{61}$$

Equation (61) describes the jump in magnetization from $m_1 = 0$ at $\tau > b/a$ to $m_1 = 1$ at $\tau < -b/a$ in the small vicinity of T_p for both qFR$_2$-qFM$_1$ and qFM$_2$-qFM$_1$ pseudotransitions.

Similarly, for the susceptibility χ_1 we may write, differentiating (59) with respect to h,

$$\chi_1 = -\frac{m_1^2}{T} + \frac{T}{\lambda_1}\frac{\partial^2\lambda_1}{\partial h^2}. \tag{62}$$

The quasisingular behavior in T_p is caused by the second term in (62). Using the same steps as in deriving (61) and leaving the main contributions, we come to the following approximations for the susceptibility near T_p,

$$\chi_1 \approx \frac{b^2}{2T_p(a^2\tau^2 + b^2)^{\frac{3}{2}}}, \tag{63}$$

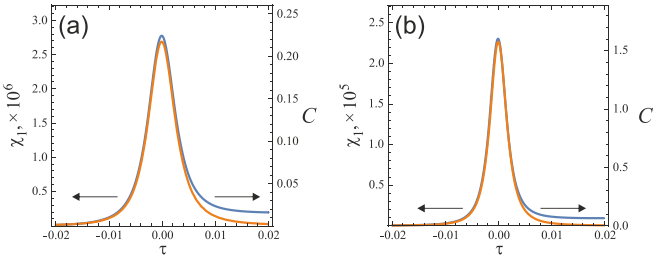

FIG. 5. The specific heat (blue line) and susceptibility (orange line) peaks in the vicinity of pseudotransition points at (a) $q = 3$, $J = -0.25$, $K = 1$, $h = -0.749995$, and (b) $q = 5$, $J = 1$, $K = 1$, $h = -0.9999$.

and its maximum value,

$$\chi_{1,p} = \frac{b^{-1}}{2T_p}. \tag{64}$$

Comparing (34) and (63), we see that dependencies of the specific heat and susceptibility in the vicinity of T_p are similar: They have the same half-width at half-maximum Ψ_τ and differ by a scale factor α, which is the ratio of the specific heat and susceptibility in the pseudotransition point

$$\alpha = \frac{C_p}{\chi_{1,p}} = a^2 T_p. \tag{65}$$

If for the qFR$_2$-qFM$_1$ pseudotransition at $q > 3$ the factor α decreases linearly with lowering T_p, for the qFR$_2$-qFM$_1$ pseudotransition at $q = 3$ and the qFM$_2$-qFM$_1$ pseudotransition, it decreases exponentially due to dependence of a. In both the latter cases, for some parameters, the giant magnitude of $\chi_{1,p}$ can be realized at the low magnitude of C_p. Indeed, for the qFR$_2$-qFM$_1$ pseudotransition at $q = 3$, we have $\chi_{1,p} \propto e^{(K-|J|)/2T_p}$, so the giant peak of susceptibility exists at sufficiently low T_p in the entire pseudotransition region defined, as it was found earlier [see Eq. (38)], by the condition $K > 3|J|$, but for the specific heat it becomes exponentially high only if $K > 5|J|$ due to Eq. (39). This case is shown in Fig. 5(a), where in the vicinity of the qFR$_2$-qFM$_1$ pseudotransition at $q = 3$, $J = -0.25$, $K = 1$, the peaks of the specific heat and susceptibility differ in amplitude by seven orders of magnitude and coincide in shape. In turn, for the qFM$_2$-qFM$_1$ pseudotransition we have $\chi_{1,p} \propto e^{(K+2J)/2T_p}$. Taking into account (40), we can conclude that the giant peak of susceptibility exists for all $J > 0$ at $K > 0$, while for the specific heat, the giant peak exists only at $0 < 2J < K$, as it follows from Eq. (41). The similarity of the specific heat and susceptibility peaks in the vicinity of the qFM$_2$-qFM$_1$ pseudotransition at $q = 5$, $J = 1$, $K = 1$, is shown in Fig. 5(b).

Temperature dependencies of the magnetic moment and susceptibility of the qFM$_1$ states near the FR$_2$-FM$_1$ boundary are shown in Fig. 6. These states both for $q = 5, J = -0.5$ and $q = 3$, $J = -0.05$ exhibit the qFR$_2$-qFM$_1$ pseudotransition with the continuous jump in the magnetic moment and the exponentially high peak of susceptibility. Figure 7 shows the magnetic moment and susceptibility for the same set of states as in Fig. 4. The dotted lines in Figs. 6(b), 6(d) 7(b), and 7(d) show approximate values of susceptibility in the pseudotransition point defined by Eq. (64).

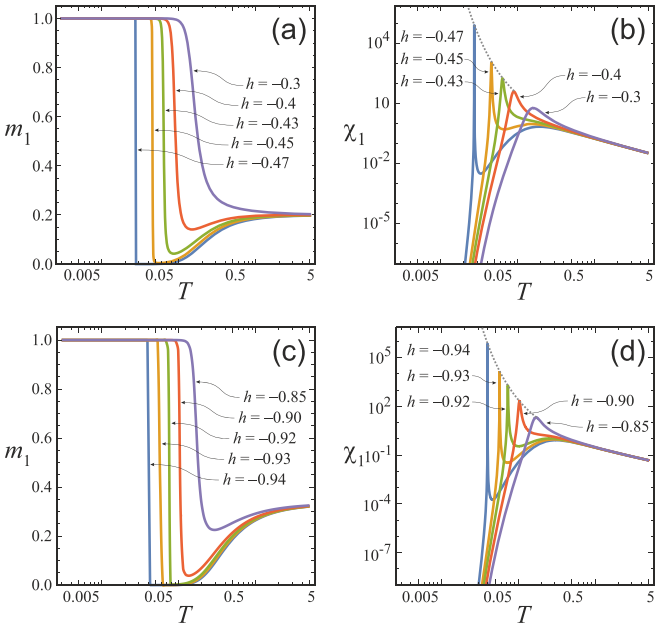

FIG. 6. The magnetic moment and susceptibility of the qFM$_1$ states near the FR$_2$-FM$_1$ boundary [(a), (b)] with $q = 5$, $J = -0.5$, $K = 1$, and [(c), (d)] with $q = 3$, $J = -0.05$, $K = 1$, in an external field h. The dotted lines in panels (b) and (d) show the magnitude of $\chi_{1,p}$ at $T = T_p$ given by Eq. (64).

Temperature dependencies of the magnetic moment and susceptibility for states near the FM$_1$-FM$_2$ boundary at $K = 0$ and $K < 0$ are shown in Fig. 8. The qualitative difference from the case $K > 0$ is seen. At $K \leqslant 0$, the magnetic moment

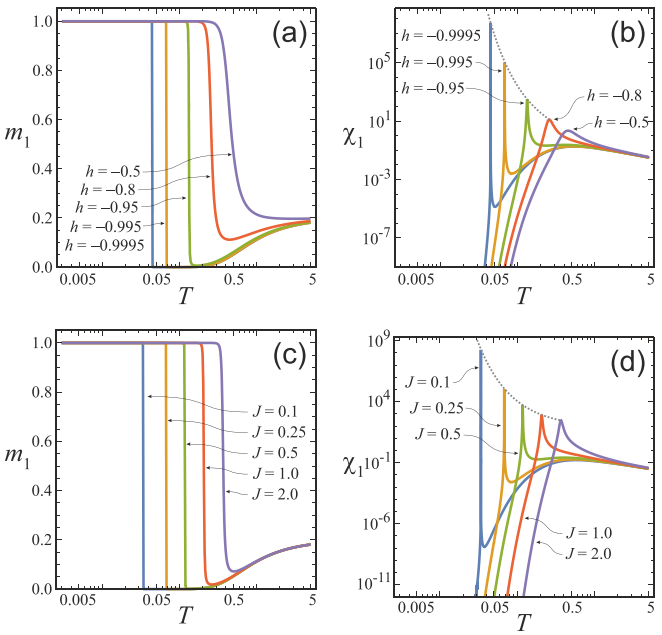

FIG. 7. The magnetic moment and susceptibility of the qFM$_1$ states near the FM$_1$-FM$_2$ boundary [(a), (b)] with $q = 5$, $J = 0.25$, $K = 1$ in an external field h, and [(c), (d)] with $q = 5$, $h = -0.995$, $K = 1$ for the different values of the coupling parameter J. The dotted lines in panels (b) and (d) show the magnitude of $\chi_{1,p}$ at $T = T_p$ given by Eq. (64).

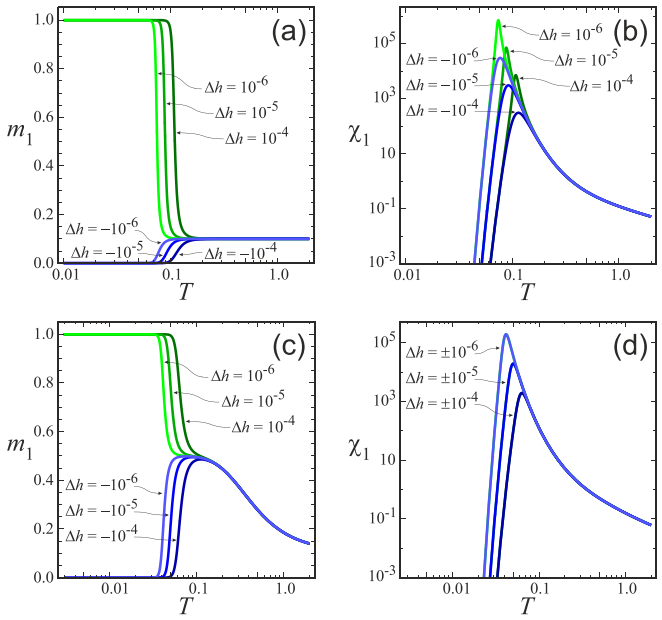

FIG. 8. The magnetic moment and susceptibility near the FM_1-FM_2 boundary for qFM_1 and qFM_2 states (green and blue lines) with $q = 10$, $J = 1$, [(a), (b)] for $K = 0$, in an external field equal to $h = \Delta h$, and [(c), (d)] for $K = -1$, in an external field equal to $h = 1 + \Delta h$.

changes with decreasing temperature from the value at the FM_1-FM_2 boundary, $m_1 = \frac{1}{q-1}$ at $K = 0$, or $m_1 = \frac{1}{2}$ at $K < 0$, to the values of the magnetic moment in the FM_1 or FM_2 phase, which are equal to 1 and 0. Because of this, the susceptibility peak is observed in both the qFM_1 and qFM_2 states.

As shown in Figs. 8(b) and 8(d), the peak of susceptibility at $K \leqslant 0$ becomes arbitrarily large in height for the qFM_1 and qFM_2 states, which are quite close to the FM_1-FM_2 boundary, but it is significantly wider compared to the case of a pseudotransition at $K > 0$, or near the qFR_2-qFM_1 pseudotransition. The extremely narrow peak, which is characteristic of a pseudotransition, exists only for $K > 0$. This follows formally from Eq. (40) and the necessary inequality $b/a \ll T_p/|J|$. The physical reason for this is the phase separation in the FM_1-FM_2 boundary at $K \leqslant 0$, which causes an intermediate value of the magnetic moment at the FM_1-FM_2 boundary and its jump in both the qFM_1 and qFM_2 states. The one-dimensional ferromagnetic Ising model has the same properties: Zero magnetization of the ground state in the absence of an external field is achieved by splitting into ferromagnetic domains with opposite magnetization, and this state represents the boundary on the phase diagram between phases with magnetizations equal to $+1$ and -1 depending on the sign of the external field. This situation can be considered as intermediate between microscopic mixing of neighboring phases at the phase boundary when there is no pseudotransition and a pure phase equal to one of the neighboring phases when the pseudotransition is realized.

IV. PAIR DISTRIBUTION CORRELATION FUNCTION

In order to accomplish our analysis, we consider the pair distribution correlation function, which is defined as follows:

$$\Gamma^{(r)}_{\mu,\mu'} = \left\langle \delta_{\sigma_i,\mu}\delta_{\sigma_{i+r},\mu'}\right\rangle - \left\langle \delta_{\sigma_i,\mu}\right\rangle\left\langle \delta_{\sigma_{i+r},\mu'}\right\rangle, \tag{66}$$

where $\Gamma^{(r)}_{\mu,\mu'} \equiv \Gamma_{\mu,\mu'}(\sigma_i, \sigma_{i+r})$.

If the system is translationally invariant, we have $\langle \delta_{\sigma_i,\mu}\rangle = \langle \delta_{\sigma_{i+r},\mu}\rangle = \langle \delta_{\sigma,\mu}\rangle = m_\mu$, and $\Gamma^{(r)}_{\mu,\mu'}$ depends only on the distance (r).

Now let us defined the average of PDF,

$$g^{(r)}_{\mu,\mu'} = \left\langle \delta_{\sigma_i,\mu}\delta_{\sigma_{i+r},\mu'}\right\rangle = \langle \boldsymbol{m}_\mu \boldsymbol{m}_{\mu'}\rangle, \tag{67}$$

so, in a natural basis it is expressed by

$$g^{(r)}_{\mu,\mu'} = Z_N^{-1}\,\mathrm{tr}(\boldsymbol{m}_\mu \mathbf{V}^r \boldsymbol{m}_{\mu'} \mathbf{V}^{N-r}), \tag{68}$$

whereas in the eigenstate basis it becomes

$$g^{(r)}_{\mu,\mu'} = Z_N^{-1}\,\mathrm{tr}(\tilde{\boldsymbol{m}}_\nu \tilde{\mathbf{V}}^r \tilde{\boldsymbol{m}}_\tau \tilde{\mathbf{V}}^{N-r}). \tag{69}$$

Writing this in terms of eigenstates,

$$g^{(r)}_{\mu,\mu'} = Z_N^{-1}\sum_{j_1=1}^{q}\langle u_{j_1}| \sum_{j_2,j_3=1}^{q} c^*_{\mu,j_2}c_{\mu,j_3}|u_{j_2}\rangle\langle u_{j_3}|\lambda^r_{j_3}$$
$$\times \sum_{j_4,j_5=1}^{q} c^*_{\mu',j_4}c_{\mu',j_5}|u_{j_4}\rangle\langle u_{j_5}|\lambda^{N-r}_{j_5}|u_{j_1}\rangle \tag{70}$$

and simplifying (70), we have

$$g^{(r)}_{\mu,\mu'} = Z_N^{-1}\sum_{j_1=1}^{q}\sum_{j_2=1}^{q} c^*_{\mu,j_1}c_{\mu,j_2}\lambda^r_{j_2}c^*_{\mu',j_2}c_{\mu',j_1}\lambda^{N-r}_{j_1}, \tag{71}$$

in the thermodynamic limit ($Z_N \to \lambda_1^N$). The above expression reduces to

$$g^{(r)}_{\mu,\mu'} = \sum_{j_1=1}^{q}\sum_{j_2=1}^{q} c^*_{\mu,j_1}c_{\mu,j_2}\left(\frac{\lambda_{j_2}}{\lambda_1}\right)^r c^*_{\mu',j_2}c_{\mu',j_1}\left(\frac{\lambda_{j_1}}{\lambda_1}\right)^{N-r}, \tag{72}$$

which by manipulating it conveniently we have

$$g^{(r)}_{\mu,\mu'} = c^*_{\mu,1}c_{\mu,1}c^*_{\mu',1}c_{\mu',1} + \sum_{j=2}^{q} c^*_{\mu,1}c_{\mu,j}\left(\frac{\lambda_j}{\lambda_1}\right)^r c^*_{\mu',j}c_{\mu',1}. \tag{73}$$

Even in terms of Eq. (43), we have

$$g^{(r)}_{\mu,\mu'} = m_\mu m_{\mu'} + c^*_{\mu,1}c_{\mu',1}\sum_{j=2}^{q} c_{\mu,j}c^*_{\mu',j}\left(\frac{\lambda_j}{\lambda_1}\right)^r. \tag{74}$$

Therefore, we can write the correlation function as follows:

$$\Gamma^{(r)}_{\mu,\mu'} = c^*_{\mu,1}c_{\mu',1}\sum_{j=2}^{q} c_{\mu,j}c^*_{\mu',j}\left(\frac{\lambda_j}{\lambda_1}\right)^r$$
$$= c^*_{\mu,1}c_{\mu',1}\left\{c_{\mu,2}c^*_{\mu',2}\left(\frac{\lambda_2}{\lambda_1}\right)^r + \left(\frac{\lambda_3}{\lambda_1}\right)^r\sum_{j=3}^{q} c_{\mu,j}c^*_{\mu',j}\right\}. \tag{75}$$

Note that for $q = 2$, the last term in (75) ceases to exist.

Taking into account the orthogonality relations for the coefficients in Eqs. (13)–(15),

$$\sum_{j=1}^{q} c_{\mu,j}c^*_{\mu',j} = \delta_{\mu,\mu'}, \tag{76}$$

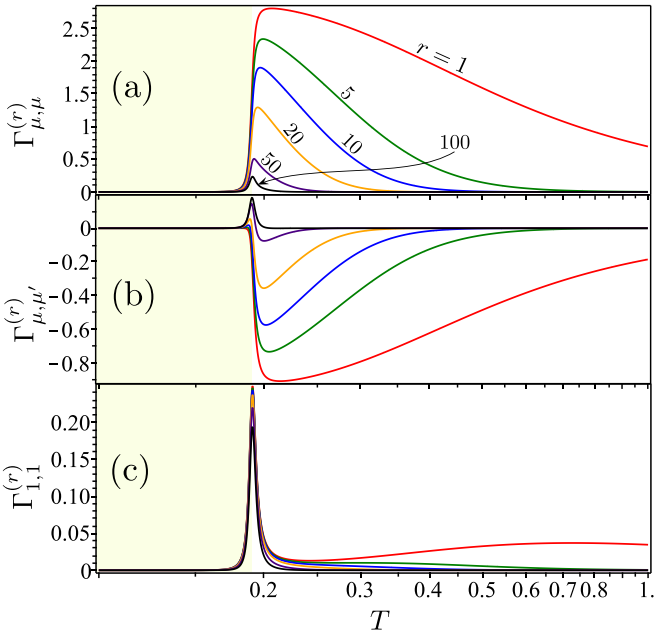

FIG. 9. The pair distribution correlation function $\Gamma^{(r)}_{\mu,\mu'}$ as a function of temperature T in logarithmic scale, assuming fixed $q = 5$, $J = 0.9$, $K = 1$, $h = -0.995$ and several values of r. (a) For $\mu = \mu'$, with $\mu = \{2, 3, \dots\}$. (b) For $\mu \neq \mu'$ with $\mu, \mu' = \{2, 3, \dots\}$. (c) For $\mu = \mu' = 1$.

(75) becomes

$$\Gamma^{(r)}_{\mu,\mu'} = c^*_{\mu,1}c_{\mu',1}\left\{c_{\mu,2}c^*_{\mu',2}\left(\frac{\lambda_2}{\lambda_1}\right)^r + \left(\delta_{\mu,\mu'} - c_{\mu,1}c^*_{\mu',1} - c_{\mu,2}c^*_{\mu',2}\right)\left(\frac{\lambda_3}{\lambda_1}\right)^r\right\}. \quad (77)$$

From (77), and after some algebraic manipulation, we can find the pair correlation functions in terms of magnetization and transfer matrix eigenvalues, which have the following form:

$$\Gamma^{(r)}_{1,1} = m_1(1-m_1)\left(\frac{\lambda_2}{\lambda_1}\right)^r, \quad (78)$$

$$\Gamma^{(r)}_{\mu,\mu} = (1-m_1)\left[m_1\left(\frac{\lambda_2}{\lambda_1}\right)^r + (q-2)\left(\frac{\lambda_3}{\lambda_1}\right)^r\right], \quad (79)$$

$$\Gamma^{(r)}_{1,\mu} = -\frac{m_1(1-m_1)}{q-1}\left(\frac{\lambda_2}{\lambda_1}\right)^r, \quad (80)$$

$$\Gamma^{(r)}_{\mu,\mu'} = (1-m_1)\left[m_1\left(\frac{\lambda_2}{\lambda_1}\right)^r - \left(\frac{\lambda_3}{\lambda_1}\right)^r\right], \quad (81)$$

where $\mu, \mu' = 2, \dots, q$ and $\mu \neq \mu'$. An alternative expression of Eqs. (78)–(81) are given in the Appendix.

In Fig. 9, we illustrate the pair correlation function $\Gamma^{(r)}_{\mu,\mu'}$ as a function of temperature in logarithmic scale, and here we consider the fixed parameters $q = 5$, $J = 0.9$, $K = 1$, $h = -0.995$ and several distances $r = \{1, 5, 10, 20, 50, 100\}$. In Fig. 9(a), we report for the case of $\mu = \mu'$ and $\mu = \{2, 3, \dots\}$, given by Eq. (79). It is worth noticing that for $T < T_p$ (enough below) this amount is closely null, meaning that the pair distribution spin orientations have no almost relationship, although for $T > T_p$ (enough above) the system exhibits clearly the relationship between pair spin orientations and as expected decreases with the distances as well as temperature. Figure 9(b) depicts the correlation function for the case $\mu \neq \mu'$ and $\mu, \mu' = \{2, 3, 4, \dots\}$, given by Eq. (81). For $T < T_p$ (enough below), the $\Gamma^{(r)}_{\mu,\mu'}$ become nearly null correlation function, while for $T > T_p$ (enough above) the systems exhibits a qualitatively different behavior, which in module decreases with r and T. Figure 9(c) displays the case of $\mu = \mu' = 1$ [according to Eq. (78)], and for this particular case we observe that the correlation function becomes almost null far enough from the pseudocritical temperature T_p, while at T_p the correlation function illustrate a peak, which decreases as expected with r. The case $\mu = 1$ and $\mu' = \{2, 3, \dots\}$ given by Eq. (81) is simply the same as the case Eq. (78) divided by $(q-1)$.

We can also notice that the four expressions given by (78)–(81) satisfy the following couple of identities:

$$\Gamma^{(r)}_{1,1} + (q-1)\Gamma^{(r)}_{1,\mu} = 0, \quad (82)$$

$$\Gamma^{(r)}_{\mu,\mu} + \Gamma^{(r)}_{1,\mu} + (q-2)\Gamma^{(r)}_{\mu,\mu'} = 0. \quad (83)$$

An equivalent expressions of the relations (82) and (83) are given in the Appendix.

Similarly, we can obtain a couple of identities for g's, by using (82) and (83), which reduce to the following relations:

$$g^{(r)}_{1,1} + (q-1)g^{(r)}_{1,\mu} = m_1, \quad (84)$$

$$g^{(r)}_{\mu,\mu} + g^{(r)}_{1,\mu} + (q-2)g^{(r)}_{\mu,\mu'} = m_\mu, \quad (85)$$

which is useful to studying the phase diagram, like illustrated in Table I.

A. Correlation length

From transfer matrix eigenvalues, one can observe that $1 > \frac{\lambda_2}{\lambda_1} > \frac{\lambda_3}{\lambda_1}$, and thus for $r > 1$, we can ignore $(\frac{\lambda_3}{\lambda_1})^r \to 0$, since $(\frac{\lambda_2}{\lambda_1})^r \gg (\frac{\lambda_3}{\lambda_1})^r$. Consequently, we can define the correlation length as follows:

$$\xi = \left[\ln\left(\frac{\lambda_1}{\lambda_2}\right)\right]^{-1}. \quad (86)$$

An approximation for the correlation length in the vicinity of the pseudotransition point immediately follows from Eq. (30) for the eigenvalues

$$\xi \approx \frac{1}{\sqrt{a^2\tau^2 + b^2}}. \quad (87)$$

At the pseudotransition point, the correlation length reaches extremely high values,

$$\xi_p = b^{-1}, \quad (88)$$

since the condition $b \ll 1$ is necessarily satisfied. Indeed, using the expressions of b in the given limit cases, we obtain

$$\xi_p = \begin{cases} \frac{1}{2}\sqrt{\frac{(q-2)x_p k_p}{q-1}} \propto e^{\frac{K-|J|}{2T_p}}, & \text{qFR}_2\text{–qFM}_1; \\ \frac{x_p}{2}\sqrt{\frac{k_p}{q-1}} \propto e^{\frac{K+2J}{2T_p}}, & \text{qFM}_2\text{–qFM}_1. \end{cases} \quad (89)$$

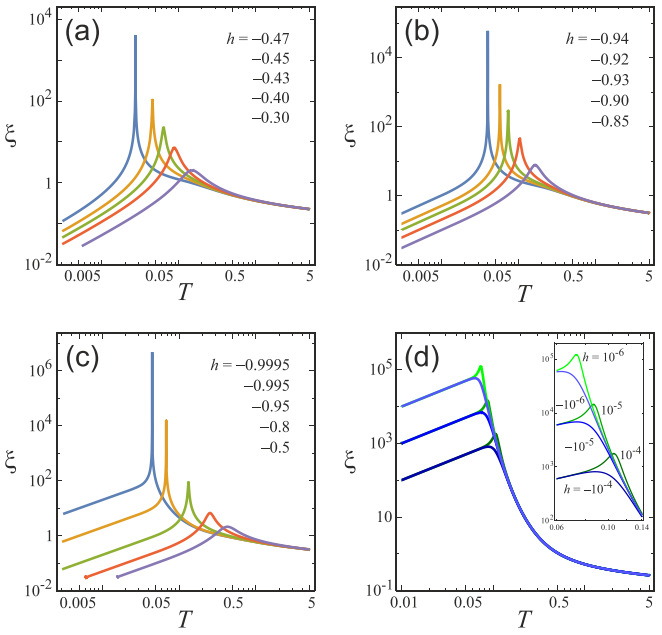

FIG. 10. The correlation length for qFM_1 states with (a) $q = 5$, $J = -0.5$, $K = 1$, (b) $q = 3$, $J = -0.05$, $K = 1$, (c) $q = 5$, $J = 0.25$, $K = 1$, and for (d) qFM_1 and qFM_2 states with $q = 10$, $J = 1$, $K = 0$, at a given h.

The half-width at half-maximum for the peak (87) of the correlation length is $\tilde{\Psi}_\tau = \sqrt{3}b/a$ and only by numeric factor differs from Ψ_τ.

Figure 10 shows the temperature dependences of the correlation length for the same sets of states as in Figs. 6(b), 6(d), 7(b), and 8(b). As for the specific heat and susceptibility, the correlation length near the pseudotransition point in Figs. 10(a)–10(c) shows the giants peaks, which are qualitatively different from other cases like shown in Fig. 10(d).

V. PSEUDOCRITICAL EXPONENTS

Now let us analyze the nature of the peaks of the specific heat, susceptibility, and correlation length around T_p and whether they follow some critical exponent universality. A general technique to calculate the critical exponents in the systems was developed in Ref. [29]. For the one-dimensional frustrated q-state Potts model, we can find these quantities directly from approximations (34), (63), and (87). Considering the region of τ where the curvature of the peaks becomes positive, $b/a < |\tau| \ll T_p/|J|$, we obtain the following asymptotics:

$$\xi = c_\xi |\tau|^{-1}, \quad c_\xi = a^{-1}, \tag{90}$$

$$C = c_f |\tau|^{-3}, \quad c_f = \tfrac{1}{2} a^{-1} b^2, \tag{91}$$

$$\chi_1 = c_\chi |\tau|^{-3}, \quad c_\chi = \frac{1}{2T_p} a^{-3} b^2. \tag{92}$$

These found critical exponents are the same as for one-dimensional models of the general class with pseudotransitions [29]. Combining the critical amplitudes, one can write

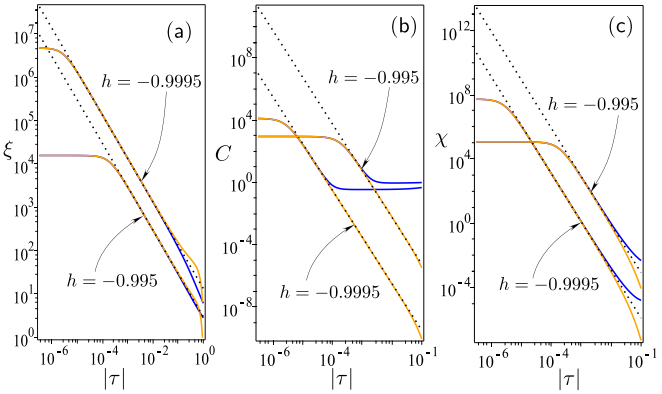

FIG. 11. (a) The correlation length as a function of $|\tau|$ in logarithmic scale, for $q = 5$, $J = 0.25$, $K = 1$, blue curves correspond to $\tau > 0$, orange curves denote the case $\tau < 0$, and dotted lines correspond to $\xi(\tau)$ in asymptotic limit. (b) The specific heat as a function of $|\tau|$ in logarithmic scale for the same set of fixed parameters in panel (a). (c) The magnetic susceptibility as a function of $|\tau|$ in logarithmic scale, for the parameters assumed in panel (a).

the following relation,

$$\frac{c_f}{c_\chi} c_\xi^2 = T_p, \tag{93}$$

which is fulfilled for all pseudotransitions in the frustrated Potts model.

In Fig. 11, we verify the power law behavior around the peak for some physical quantities; these results are only valid for the ascending and descending parts of the peak, while this approach fails around the top of the peak. In Fig. 11(a), we report the correlation length as a function of $|\tau|$ in logarithmic scale assuming the parameters $q = 5$, $J = 0.25$, $K = 1$. Blue curves correspond for $\tau > 0$, orange curves denote for $\tau < 0$, and dotted lines describe the asymptotic behavior given by Eq. (90). We consider two values of the magnetic field as indicated in Fig. 11(a). For $h = -0.995$, we can observe clearly a straight line with pseudocritical exponent $\nu = 1$ in a range of $10^{-4} \lesssim \tau \lesssim 10^{-1}$ (blue curve). Such behavior we also observe for the case $-10^{-1} \lesssim \tau \lesssim -10^{-4}$ (orange curve). Note that for $|\tau| \lesssim 10^{-4}$ the asymptotic behavior fails because it corresponds to the peak of the curve. Similar behavior is illustrated for $h = -0.9995$ and the pseudocritical exponent is accurately described by a straight line with the same exponent $\nu = 1$, although the asymptotic approach is valid roughly in the interval $10^{-1} \lesssim |\tau| \lesssim 10^{-6}$. Figure 11(b) depicts the specific heat as a function of $|\tau|$ in logarithmic scale, assuming the same fixed parameters as those considered in Fig. 11(a), where the specific heat also exhibits a descending part of the peak as a straight line, which fits precisely to a straight dotted line with angular coefficient $\alpha = 3$ given by Eq. (91), although in the shorter interval and for smaller $|\tau|$, the straight lines fail for $|\tau| \lesssim 10^{-5}$ ($h = -0.9995$) and $|\tau| \lesssim 5 \times 10^{-3}$ ($h = -0.995$) because we are dealing with a peak and not a real singularity. Analogous behavior is observed for the magnetic susceptibility in Fig. 11(c), assuming the same set of fixed parameters given in Fig. 11(a). Once again, we observe clearly a straight line with angular coefficient $\mu = 3$ given by Eq. (92), which is valid for a wider interval compared to that of specific heat.

In summary, the pseudocritical exponents are independent of the magnetic field. We also conclude that these exponents satisfy the same universality class found previously for other one-dimensional models.

VI. CONCLUSION

Although one-dimensional systems could appear to be thoroughly studied, they still surprise us by exhibiting unconventional physics. There are some peculiar one-dimensional models that exhibit the presence of phase transition at finite temperature under the condition of nearest-neighbor interaction [21–26]. One-dimensional models of statistical physics are attractive from both theoretical and experimental points of view for developing new methods to solve more realistic models.

Here we investigated more carefully the one-dimensional Potts model with an external magnetic field and anisotropic interaction that selects neighboring sites that are in the spin state 1, by using the transfer matrix method. The largest and second largest eigenvalues are almost degenerate for a given temperature, leading to pseudotransition. The rise of anomalous behavior in this model is caused by the peculiar behavior of the transfer matrix elements: All transfer matrix elements are positive, but some off-diagonal matrix in the low-temperature region can be extremely small compared to at least two diagonal elements. We have analyzed the present model for several physical quantities assuming $K = 1$. The entropy and magnetization show a steep function around pseudocritical temperature, similar to a first-order phase transition, while the correlation length, specific heat, and magnetic susceptibility exhibit sharp peaks around pseudocritical temperature, resembling a second-order phase transition, although there is no true divergence. A further investigation of the pseudocritical exponent satisfies the same class of universality previously identified for other one-dimensional models; these exponents are for correlation length $\nu = 1$, specific heat $\alpha = 3$ and magnetic susceptibility $\mu = 3$. For $K = 0$ (standard Potts chain), we observe a qualitatively different behavior, such as in entropy there is no steplike function, there is no sharp peak in specific heat, and a broad peak arises for magnetic susceptibility.

It is worth mentioning that the pseudotransition is quite different from a true phase transition because there is no jump in the first derivative of free energy nor divergence in the second derivative of free energy. In this sense, it would be fairly relevant to observe this anomalous property experimentally in chemical compounds.

ACKNOWLEDGMENTS

The work was partly supported by the Ministry of Education and Science of the Russian Federation, Project No. FEUZ-2020-0054, and Brazilian agencies CNPq and FAPEMIG.

APPENDIX: SOME ADDITION RELATIONS

Here we give some additional alternative expressions, which would be useful for further analysis. Equations (78)–(81) can be reduced to

$$\Gamma^{(r)}_{1,1} = \frac{\sin^2(2\phi)}{4}\left(\frac{\lambda_2}{\lambda_1}\right)^r, \tag{A1}$$

$$\Gamma^{(r)}_{\mu,\mu} = \frac{\Gamma^{(r)}_{1,1}}{(q-1)^2} + \frac{(q-2)\sin^2(\phi)}{(q-1)^2}\left(\frac{\lambda_3}{\lambda_1}\right)^r, \tag{A2}$$

$$\Gamma^{(r)}_{1,\mu} = -\frac{\Gamma^{(r)}_{1,1}}{q-1}, \tag{A3}$$

$$\Gamma^{(r)}_{\mu,\mu'} = \frac{\Gamma^{(r)}_{1,1}}{(q-1)^2} - \frac{\sin^2(\phi)}{(q-1)^2}\left(\frac{\lambda_3}{\lambda_1}\right)^r. \tag{A4}$$

Considering the identities given by (82) and (83), we obtain the following identity which must satisfy

$$\Gamma^{(r)}_{1,1} + (q-1)\Gamma^{(r)}_{\mu,\mu} + 2(q-1)\Gamma^{(r)}_{1,\mu} + (q-1)(q-2)\Gamma^{(r)}_{\mu,\mu'} = 0. \tag{A5}$$

An equivalent relation we can verify, so the pair average distribution functions obey the identity

$$g^{(r)}_{1,1} + (q-1)g^{(r)}_{\mu,\mu} + 2(q-1)g^{(r)}_{1,\mu} + (q-1)(q-2)g^{(r)}_{\mu,\mu'} = 1. \tag{A6}$$

Below we simplify for the nearest-neighbor PDF $g^{(1)}_{\mu,\mu'}$, which can be written as

$$g^{(1)}_{1,1} = \frac{(\lambda_1 - \lambda_3 - (q-1)t_2)(\lambda_1 + \lambda_2 - \lambda_3 - (q-1)t_2)}{\lambda_1(\lambda_1 - \lambda_2)}, \tag{A7}$$

$$g^{(1)}_{\mu,\mu} = \frac{(\lambda_3 + t_2)(\lambda_3 - \lambda_2 + (q-1)t_2)}{(q-1)\lambda_1(\lambda_1 - \lambda_2)}, \tag{A8}$$

$$g^{(1)}_{1,\mu} = \frac{(\lambda_1 - \lambda_3 - (q-1)t_2)(\lambda_3 - \lambda_2 + (q-1)t_2)}{(q-1)\lambda_1(\lambda_1 - \lambda_2)}, \tag{A9}$$

$$g^{(1)}_{\mu,\mu'} = \frac{(\lambda_3 - \lambda_2 + (q-1)t_2)t_2}{(q-1)\lambda_1(\lambda_1 - \lambda_2)}, \tag{A10}$$

where $\mu, \mu' = 2, \ldots q$, and $\mu \neq \mu'$. These amounts are useful to analyze the phase boundary properties illustrated in Table I.

[1] R. J. Baxter, *Exactly Solved Models in Statistical Mechanics* (Academic Press, London, 1982).
[2] R. G. Ghulghazaryan, K. G. Sargsyan, and N. S. Ananikian, Phys. Rev. E **76**, 021104 (2007).
[3] V. Hovhannisyan, R. Ghulghazaryan, and N. Ananikian, Phys. A (Amsterdam, Neth.) **388**, 1479 (2009).
[4] L. van Hove, Phys. (Amsterdam, Neth.) **16**, 137 (1950).
[5] F. Ninio, J. Phys. A: Math. Gen. **9**, 1281 (1976).

[6] J. A. Cuesta and A. Sánchez, J. Stat. Phys. **115**, 869 (2004).
[7] C. Kittel, Am. J. Phys. **37**, 917 (1969).
[8] S. T. Chui and J. D. Weeks, Phys. Rev. B **23**, 2438 (1981).
[9] T. Dauxois and M. Peyrard, Phys. Rev. E **51**, 4027 (1995).
[10] P. Sarkanych, Y. Holovatch, and R. Kenna, Phys. Lett. A **381**, 3589 (2017).
[11] B. H. Zimm and J. K. Bragg, J. Chem. Phys. **31**, 526 (1959).
[12] A. V. Badasyan, A. Giacometti, Y. S. Mamasakhlisov, V. F. Morozov, and A. S. Benight, Phys. Rev. E **81**, 021921 (2010).
[13] N. S. Ananikyan, S. A. Hajryan, E. S. Mamasakhlisov, and V. F. Morozov, Biopolymers **30**, 357 (1990).
[14] A. Badasyan, A. Giacometti, R. Podgornik, Y. Mamasakhlisov, and V. Morozov, Eur. Phys. J. E **36**, 46 (2013).
[15] S. Tonoyan, D. Khechoyan, Y. Mamasakhlisov, and A. Badasyan, Phys. Rev. E **101**, 062422 (2020).
[16] F. Y. Wu, Rev. Mod. Phys. **54**, 235 (1982).
[17] A. Aharony and P. Pfeuty, J. Phys. C **12**, L125 (1979).
[18] T. C. Lubensky and J. Isaacson, Phys. Rev. Lett. **41**, 829 (1978).
[19] C. M. Chaves and R. Riera, Can. J. Phys. **62**, 69 (1984).
[20] Y. Panov, J. Magn. Magn. Mater. **514**, 167224 (2020).
[21] L. Gálisová and J. Strečka, Phys. Rev. E **91**, 022134 (2015).
[22] L. Gálisová, Phys. Rev. E **96**, 052110 (2017); Acta Phys. Pol. A **137**, 604 (2020).
[23] J. Strečka, R. C. Alécio, M. L. Lyra, and O. Rojas, J. Magn. Magn. Mater. **409**, 124 (2016).
[24] O. Rojas, J. Strečka, and S. de Souza, Solid State Commun. **246**, 68 (2016).
[25] J. Strečka, Acta Phys. Pol. A **137**, 610 (2020).
[26] S. de Souza and O. Rojas, Solid State Commun. **269**, 131 (2018).
[27] I. Carvalho, J. Torrico, S. de Souza, O. Rojas, and O. Derzhko, Ann. Phys. **402**, 45 (2019).
[28] O. Rojas, Acta Phys. Pol. A **137**, 933 (2020); Braz. J. Phys. **50**, 675 (2020).
[29] O. Rojas, J. Strečka, M. L. Lyra, and S. M. de Souza, Phys. Rev. E **99**, 042117 (2019).
[30] W. Janke and A. M. Schakel, Nucl. Phys. B **700**, 385 (2004).
[31] X. Qian, Y. Deng, and H. W. J. Blöte, Phys. Rev. E **72**, 056132 (2005).